# Correction

**NEUROSCIENCE**

Correction for "Nitric oxide regulates synaptic transmission between spiny projection neurons," by Yotam Sagi, Myriam Heiman, Jayms D. Peterson, Sergei Musatov, Michael G. Kaplitt, Dalton J. Surmeier, Nathaniel Heintz, and Paul Greengard, which appeared in issue 49, December 9, 2014, of *Proc Natl Acad Sci USA* (111:17636–17641; first published November 20, 2014; 10.1073/pnas.1420162111).

The authors note that Mariangela Scarduzio and Stephen M. Logan should be added to the author list between Sergei Musatov and Michael G. Kaplitt. Mariangela Scarduzio should be listed as the fifth author and Stephen M. Logan should be listed as the sixth author. Both Mariangela Scarduzio and Stephen M. Logan should be credited with performing research. The corrected author line, affiliation line, and author contributions appear below. The online version has been corrected.

**Yotam Sagi[a,1], Myriam Heiman[a,2], Jayms D. Peterson[b], Sergei Musatov[c], Mariangela Scarduzio[b], Stephen M. Logan[b], Michael G. Kaplitt[c], Dalton J. Surmeier[b], Nathaniel Heintz[d,e], and Paul Greengard[a,1]**

[a]Laboratory of Molecular and Cellular Neuroscience, The Rockefeller University, New York, NY 10065; [b]Department of Physiology, Northwestern University Feinberg School of Medicine, Chicago, IL 60611; [c]Laboratory of Molecular Neurosurgery, Weill Medical College of Cornell University, New York, NY 10065; and [d]Laboratory of Molecular Biology and [e]Howard Hughes Medical Institute, The Rockefeller University, New York, NY 10065

Author contributions: Y.S., M.H., J.D.P., D.J.S., and P.G. designed research; Y.S., J.D.P., M.S., and S.M.L. performed research; S.M., M.G.K., and N.H. contributed new reagents/analytic tools; Y.S. and J.D.P. analyzed data; Y.S., M.H., J.D.P., D.J.S., and P.G. wrote the paper; and M.G.K. provided tools and guidance on methods used in this work.

**CORRECTION**

# Nitric oxide regulates synaptic transmission between spiny projection neurons

Yotam Sagi[a,1], Myriam Heiman[a,2], Jayms D. Peterson[b], Sergei Musatov[c], Mariangela Scarduzio[b], Stephen M. Logan[b], Michael G. Kaplitt[c], Dalton J. Surmeier[b], Nathaniel Heintz[d,e], and Paul Greengard[a,1]

[a]Laboratory of Molecular and Cellular Neuroscience, The Rockefeller University, New York, NY 10065; [b]Department of Physiology, Northwestern University Feinberg School of Medicine, Chicago, IL 60611; [c]Laboratory of Molecular Neurosurgery, Weill Medical College of Cornell University, New York, NY 10065; and [d]Laboratory of Molecular Biology and [e]Howard Hughes Medical Institute, The Rockefeller University, New York, NY 10065

Recurrent axon collaterals are a major means of communication between spiny projection neurons (SPNs) in the striatum and profoundly affect the function of the basal ganglia. However, little is known about the molecular and cellular mechanisms that underlie this communication. We show that intrastriatal nitric oxide (NO) signaling elevates the expression of the vesicular GABA transporter (VGAT) within recurrent collaterals of SPNs. Down-regulation of striatal NO signaling resulted in an attenuation of GABAergic signaling in SPN local collaterals, down-regulation of VGAT expression in local processes of SPNs, and impaired motor behavior. PKG1 and cAMP response element-binding protein are involved in the signal transduction that transcriptionally regulates VGAT by NO. These data suggest that transcriptional control of the vesicular GABA transporter by NO regulates GABA transmission and action selection.

guanylyl cyclase | vesicular GABA transporter | BacTRAP | spiny projecting neurons | axon collaterals

Throughout the CNS, the volume transmitter nitric oxide (NO) has been implicated in modulating synaptic function, including transmitter release and plasticity (1, 2). The primary target of NO is soluble guanylyl cyclase (sGC), a heterodimer comprising α and β subunits. Upon activation, sGC generates the intracellular messenger cGMP, which, in turn, regulates downstream targets, including channels, phosphodiesterases, and kinases, to alter synaptic function (3). Although sGC is expressed in many adult brain areas, its expression level and activity are highest in the striatum (4, 5), where it is thought to facilitate NO-mediated transmission and plasticity at cortico-striatal synapses (6, 7).

To identify plasticity-related molecules that are regulated by NO signaling in striatal neurons, we generated striatal-specific sGCβ1 knockdown (KD) mice and analyzed the resulting transcriptional alterations in a defined population of spiny projection neurons (SPNs). We demonstrated reduction in the levels of the vesicular GABA transporter (VGAT) and GABA signaling at recurrent axon collaterals of striatal SPNs. Signaling between SPNs was also attenuated by pharmacological inhibition of NO signaling. The transcriptional regulation of VGAT by cGMP involved phosphorylation of cAMP response element-binding protein (CREB) by cGMP-dependent protein kinase G (PKG). Our data indicate that NO signaling modulates neurotransmission at neural circuits by modulating the transcription of the vesicular GABA transporter.

## Results

### Biochemical and Behavioral Characterization of Striatal-sGCβ1 KD Mice.
We generated striatal sGCβ1 KD mice to identify the cellular processes regulated by NO specifically in striatal neurons of the adult brain, while avoiding its roles in glutamate nerve terminals, nonneuronal cells, or during neuronal development. For this siGucy, shRNA against *Gucy1b3* (the gene encoding sGCβ1) was inserted into an AAV2-delivery system, and its activity was first evaluated in cortical neuron culture. AAV.siGucy or control

AAV (AAV.siLuc) were transduced into $87.1 \pm 2.13\%$ and $89.7 \pm 1.84\%$ of the neurons in the culture, respectively. AAV.siGucy, but not AAV.siLuc, reduced endogenous sGCβ1 levels by $44 \pm 12\%$ (Fig. 1 A and B) and attenuated NO-induced production of cGMP by $95 \pm 2\%$ (Fig. 1C). Stereotaxic delivery of the virus into the dorsal striatum of adult mice resulted in specific localization of GFP throughout the entire striatum (Fig. 1D), but not the cortex, indicating that corticostriatal neurons were not targeted by the virus. In striata transduced with either AAV.siGucy or AAV.siLuc, over 90% of the GFP-labeled cells were also positive for the 32-kDa dopamine- and cyclic AMP-regulated phosphoprotein (DARPP-32), suggesting that SPNs are the primary target of these viruses (Fig. S1). Notably, AAV.siGucy delivery resulted in a $37 \pm 7\%$ reduction of striatal sGCβ1 level (Fig. 1 E and F). In line with this result, we found that sGC activity was dramatically reduced in sGCβ1 KD mice, as reflected by an $82 \pm 8\%$ reduction in endogenous striatal cGMP level (Fig. 1G). Interestingly, cAMP levels were not changed in either cultured neurons transduced with AAV.siGucy or in sGCβ1 KD mice, suggesting that its hydrolysis in the striatum is not regulated by cGMP (Fig. 1 C and G).

Basal motor behavior of sGCβ1 KD mice was evaluated using the open-field test. sGCβ1 KD mice had higher motor activity relative to control (Fig. 1H). The induction of motor behavior in sGC-KD mice was not detected in the first 5 min of the test (sGCβ1 KD vehicle $714 \pm 76$ cm; control $621 \pm 95$ cm; $P = 0.12$) (Fig. 1I) whereas acute administration of the nitric oxide synthase inhibitor L-NG-nitroarginine methyl ester, (L-NAME) to sGCβ1 KD mice attenuated movement ($90 \pm 20$ cm) as previously shown in WT (8, 9), suggesting that extrastriatal NOS are

### Significance

The function of the basal ganglia relies on striatal spiny projecting neurons (SPNs). Axon collaterals of these GABAergic neurons form connections with other SPNs as a means of a feedback inhibition circuit. The mechanisms that regulate neurotransmission at these local synapses remain poorly understood. In this paper, neurotransmission at SPN collaterals is found to be regulated by the gaseous neurotransmitter nitric oxide, which activates a signal-transduction cascade that transcriptionally regulates vesicular GABA transporter specifically at axon collaterals. These findings illustrate a previously unidentified role for nitric oxide in striatal learning and action selection.
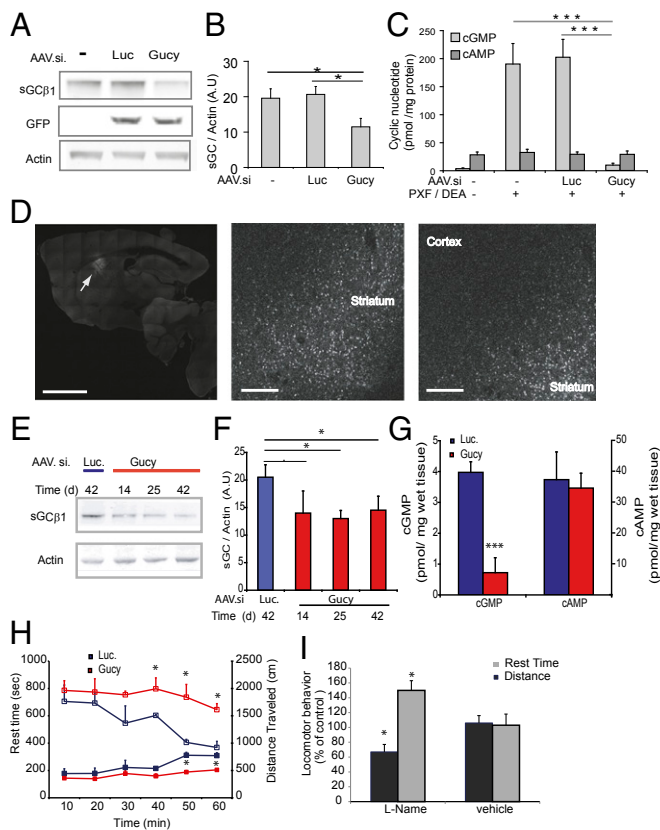
**Fig. 1.** Biochemical and behavioral impairments in striatal-sGCβ1 KD mice. (A) Representative Western blot images depicting endogenous sGCβ1, transduced GFP, and β-actin levels in cortical culture neurons untreated (n = 3 wells) or transduced with either AAV.siGucy (n = 3 wells) or the control virus, AAV.siLuc (n = 3 wells). (B) Bar graph summary of the data presented in A. Bars represent mean sGCβ1 levels normalized to β-actin ± SD. (C) Effect of the nitric oxide donor, diethylamine NONOate (DEA, 10 nM) and a phosphodiesterase inhibitor, pentoxifylline (PXF, 150 μM) on cGMP and cAMP levels in neuron culture (n = 3 for each condition, ***P < 0.001). Bars represent means ± SD. (D) Representative grayscale immunofluorescent images of GFP localization after intrastriatal injection of AAV.siGucy, showing GFP expression in the dorsal striatum (arrow, *Left*). Magnified images (*Middle* and *Right*) show the somatic GFP labeling throughout the striatum. (Scale bars: *Left*, 2 mm, objective 10×; *Middle* and *Right*, 200 μm, objective 40×.) (E) Representative Western blot image of protein level from lysates of the entire striata after bilateral intrastriatal injections of either AAV.siGucy or control AAV (AAV.siLuc, n = 4 mice per group, for coordinates see *SI Materials and Methods*). (F) Quantification of the data presented in E, indicating a persistent reduction in sGCβ1 level by AAV.siGucy (*P < 0.05). Bars represent mean densities of sGCβ1 normalized to β-actin ± SD. (G) Quantification of cGMP and cAMP levels in control or sGCβ1 KD (n = 6 mice per group, ***P = 0.0004). Bars represent levels normalized to tissue wet weight ± SD. (H) Spontaneous motor behavior was recorded for 60 min after vehicle injection. Traveled distance and rest times are illustrated by the open and closed boxes, respectively (n = 6 mice per group, *P < 0.05). (I) Five-minute motor activity in sGCβ1 KD mice was compared with that of mice injected with the nitric synthase inhibitor L-NG-nitroarginine methyl ester (L-NAME) (n = 6 mice per group, *P < 0.05 vs. untreated control).

the target of the drug. Taken together, these results suggest that striatal NO signaling regulates motor function.

**Striatal VGAT Is Down-Regulated in SPNs of sGCβ1 KD Mice.** Accumulating data indicate that striatal NO signaling regulates synaptic plasticity (6, 7). We therefore hypothesized that the behavioral impairments in sGCβ1 KD mice are mediated by altering expression of proteins related to plasticity. To identify the genes regulated by NO signaling, we analyzed the translated

mRNA expression profile of SPNs from sGCβ1 KD mice. To this end, we used the newly developed translating ribosome affinity purification (TRAP) system (10, 11) and isolated translated mRNA from SPNs of the direct projection pathway (dSPNs). qPCR analysis corroborated a 41 ± 18% reduction in sGCβ1 mRNA in Drd1-expressing SPNs of sGCβ1 KD mice, confirming that SPNs are the target of the AAV (Fig. 2A). We next compared the expression level of ~14,000 genes from dSPNs of sGCβ1 KD-Drd1-TRAP mice to that from mice injected with the control virus. Of the probe sets, 2.7% were down-regulated in dSPNs of sGCβ1 KD mice and 7.5% were induced, compared with control, but none of these genes are associated with glutamatergic signaling. In contrast, among the genes showing the most prominent change was the vesicular GABA transporter (VGAT, *Slc32a1*), which was reduced by 38 ± 6% in sGCβ1 KD relative to control (Table S1). Of all annotated synaptic vesicle-related genes, 13.5% were differentially regulated in SPNs of sGCβ1 KD, including *stx3, stx7, dept7, syt12, rab9b, kif2a, kif2c, kif3b, kif3c, kif5b, kif13a, kif17, kif21a, stxbp1, pi3kr1, pi3kc1, vamp4,* and *vamp7* (Table S1). However, none of these genes are functionally related to VGAT, suggesting that the transcriptional regulation of VGAT by NO signaling is selective and not part of a complete reorganization in the synaptic vesicle-related proteins. qPCR analysis corroborated a 43 ± 15% reduction in VGAT-translated mRNA in dSPN of sGCβ1 KD mice (Fig. 2A).

NO signaling has been implicated in modulating the function of local synapses of SPNs as well as primary projections of dSPNs
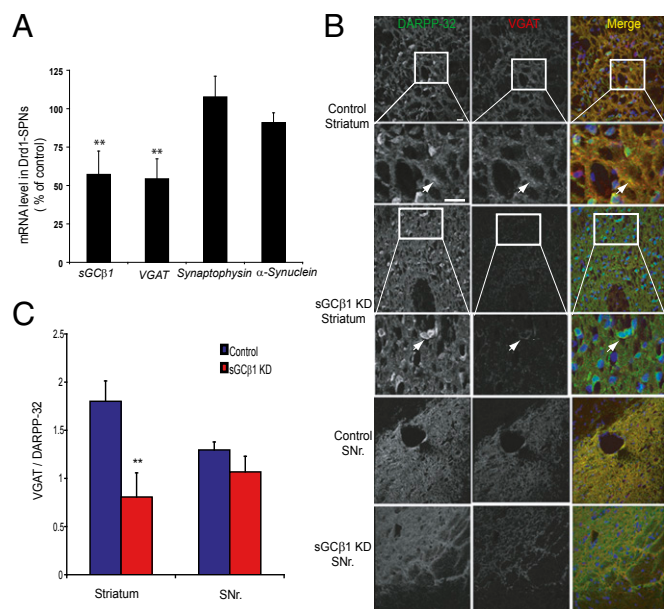


**Fig. 2.** VGAT is down-regulated in local processes of striatal SPNs in sGCβ1 KD mice. (A) Bar graph summary of mRNA levels of sGCβ1 (*gucy1b3*), VGAT (*Slc32a1*), synaptophysin (*Syp*), and α-synuclein (*Snca*) from control Drd1-TRAP mice and sGCβ1 KD Drd1-TRAP mice (n = 3 per group, **P < 0.01 vs. control). Bars represent mean mRNA levels normalized to GAPDH, as percentage of control ± SD. (B) Colocalization of VGAT and DARPP-32 in the striatum and substantia nigra pars reticulata (SNr). Representative images from control (n = 5 mice), showing that VGAT is colocalized with DARPP-32 in the striatum. Note in the magnified images that VGAT is expressed in the soma (adjacent to the nucleus in blue) but more prominently in processes (arrows) of SPNs. In sGCβ1 KD (n = 5 mice), VGAT labeling is mainly reduced in processes but it is still visible in somas (arrows). In control mice, SPNs' principal projections to the SNr express VGAT, and the labeling of VGAT in the principal projection remains unchanged in sGCβ1 KD mice. (Scale bar: 20 μm.) (C) Mean pixel values were determined concomitantly for DARPP-32 and VGAT in control (n = 5 mice) and sGCβ1 KD mice (n = 5 mice). Analysis of the ratios indicates that VGAT level is reduced in the striatum of sGCβ1 KD mice (**P = 0.0095). Bars represent mean ratios of mean pixel values ± SEM.

to the substantia nigra pars reticulata (SNr) (6, 12). To analyze the cellular localization of VGAT in SPNs of sGCβ1 KD mice, brain sections were costained for VGAT and DARPP-32. In the striatum, VGAT was highly but not completely localized in SPNs (Fig. 2B), with a more prominent localization to neuropil, relative to perikarya, indicating its presence in recurrent axon collaterals. Consistent with the reduction in mRNA level, VGAT-protein labeling was 55 ± 15% in the striatum of sGCβ1 KD relative to control mice (Fig. 2 B and C). We next compared the level of VGAT in dSPNs and indirect projection SPNs (iSPNs), by analyzing VGAT and GFP immunolabeling in sGCβ1 KD-Drd1-TRAP mice. In line with the TRAP data, the VGAT level in Drd1-positive cells of sGCβ1 KD mice was reduced by 32 ± 5.3% and in Drd1-negative neurons by 25 ± 8.5%, relative to their respective controls (Fig. S2). In contrast to the reduction in the immunolabeling of VGAT in SPNs, VGAT labeling in interneurons of these mice was unchanged (Fig. S3), suggesting that NO signaling regulates VGAT expression in both dSPNs and iSPNs.

## GABA Transmission at Recurrent Collaterals of SPNs Is Impaired in sGCβ1 KD Mice.

To evaluate the role of sGC on GABA transmission in SPNs, GABA miniature inhibitory postsynaptic currents (mIPSCs) were recorded in SPNs. GABA mIPSC frequency was 25 ± 8% lower in SPNs taken from sGCβ1 KD mice compared with controls (Fig. 3 B and C), suggesting a decrease in the release probability of GABAergic synapses onto SPNs (13). Visual inspection of representative records suggested that the frequency of small-amplitude mIPSCs was selectively decreased in SPNs of sGCβ1 KD mice (Fig. 3A). This finding was confirmed by a quantitative analysis of the amplitude distribution of mIPSCs from equal-length records (Fig. 3D). The distribution analysis revealed a 29 ± 8% reduction in the number of mIPSCs with amplitudes less than 65 pA, but not mIPSCs with amplitudes greater than 65 pA (Fig. 3E). The alterations in frequency and amplitude were not accompanied by a significant change in mIPSC kinetics (Fig. 3 F and G), suggesting that GABAergic synapses were not being redistributed. GABAergic synapses onto SPNs are derived from one of three sources: fast-spiking (FS) interneurons, neuronal nitric oxide synthase (nNOS)-positive interneurons, and collateral SPN synapses (14, 15). FS interneurons make perisomatic synapses that give rise to large-amplitude IPSCs. In contrast, nNOS interneurons and SPN synapse primarily upon dendrites and give rise to small-amplitude IPSCs. Because SPNs far outnumber nNOS interneurons, it seems likely that the drop in the frequency of small-amplitude mIPSCs in sGCβ1 KD mice is attributable to a reduction in GABA release from recurrent collaterals.

To physiologically evaluate the function of VGAT in the efferents of dSPNs of sGCβ1 KD mice, the paired pulse ratio of IPSCs in SNr neurons was studied. Striatonigral IPSCs were strongly facilitated and were not altered in sGCβ1 KD mice (Fig. S4), suggesting that GABA transmission at extrastriatal terminals of SPNs was unchanged.

To determine whether NO signaling directly modulates recurrent collateral synapses, recurrent collaterals of the indirect pathway were activated optogenetically while recording from a dSPN, (Fig. 4 A and B). The IPSCs evoked by collateral activation were significantly diminished by disruption of NOS signaling with L-NAME (100 μM) (Fig. 4 C and D). This result demonstrates that NO signaling potentiates recurrent collateral GABAergic synaptic function, in agreement with the inference drawn from the mIPSC analysis.

## PKG1 and CREB Mediate the Transcriptional Regulation of VGAT by NO.

To elucidate the signaling pathway involved in the transcriptional regulation of VGAT by NO, the phosphorylation level of phosphoproteins involved in striatal and NO signaling, including DARPP-32, ERK1/2, and CREB (6, 16, 17), was assessed. In the striatum, the phosphorylation level of serine 133-CREB was reduced by 62 ± 19% in sGCβ1 KD mice compared
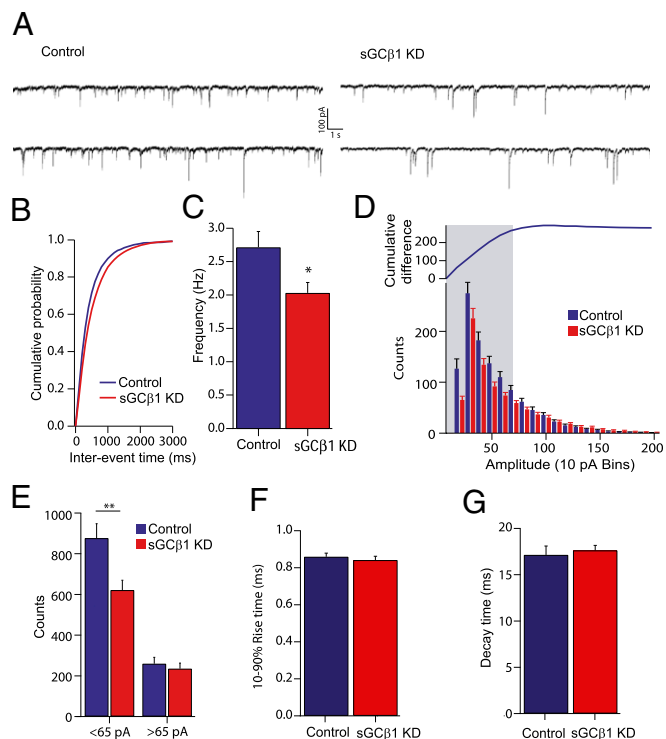


**Fig. 3.** Decreased frequency of small-amplitude GABAergic currents in striatal SPNs of sCGβ1 KD mice. (A) Representative spontaneous mIPSC traces from SPNs of control (n = 18 mice) and sGCβ1 KD (n = 19 mice). (B) Cumulative probability plot summary of mIPSC interevent interval (IEI) from control or sGCβ1 KD, showing an increase in IEI in SPNs of sGCβ1 KD mice. (C) Bar graph summary of mIPSC frequency in SPNs from control (n = 18 mice) or sGCβ1 KD (n = 19 mice), showing a decrease in SPN mIPSCs frequency in sGCβ1 KD animals (*P = 0.022). Bars represent mean frequency ± SEM. (D, Lower) Amplitude histogram of mIPSCs in SPNs of control (n = 18 mice) and sGCβ1 KD (n = 19 mice) showing a decrease in the number of mIPSCs in the smaller amplitude event bins in sGCβ1 KD mice. (Upper) Cumulative plot of the difference between control (n = 18 mice) and sGCβ1 KD (n = 19 mice) in each 10-pA-amplitude bin, showing that the greatest difference between the groups occurs in the smaller amplitude bins. (E) Bar graph summary of small (<65 pA) and big (>65 pA) amplitude mIPSCs in equal-length records (7 min) from control (n = 18 mice) or sGCβ1 KD (n = 19 mice), showing a decrease in the number of small-amplitude mIPSCs in SPNs of sGCβ1 KD (**P = 0.006). Bars represent mean counts ± SEM. (F) Bar graph summary of mean 10–90% rise times (P = 0.524, control, 0.86 ± 0.02, n = 19; sGCβ1 KD, 0.84 ± 0.02, n = 18). (G) Mean decay times (P = 0.664, control, 17.1 ± 1.0, n = 19; sGCβ1 KD, 17.6 ± 0.5, n = 18).

with control mice (Fig. 5 A and B), supporting the idea that CREB plays a role in the transcriptional regulation of VGAT by NO. In contrast to CREB, the phosphorylation levels of threonine 202/tyrosine 204-ERK1/2, and threonine 34-DARPP-32 of sGCβ1 KD mice were 118 ± 9% and 94 ± 13% of the respective control (Fig. 5 A and B). We next studied whether CREB phosphorylation is dependent on cGMP and cGMP-dependent kinase (PKG)1 in striatal slices. We found a 150 ± 22% increase in CREB phosphorylation after cGMP bath application (Fig. 5 C and D). PKG1 has an established role in directly phosphorylating CREB, and this activity may depend on nuclear shuttling of PKG1 (18). In line with this result, the effect of cGMP was completely abolished by PKG1 inhibition (106 ± 15% of basal phosphorylation level) (Fig. 5 C and D). To identify the subcellular localization of PKG1 after activation by cGMP, the cytoplasmic and nuclear protein fractions were separated. At basal level, PKG1 was localized to both nuclear and cytoplasmic compartments of striatal cells, and cGMP-induced phosphorylation of CREB by PKG1 was not associated with changes in
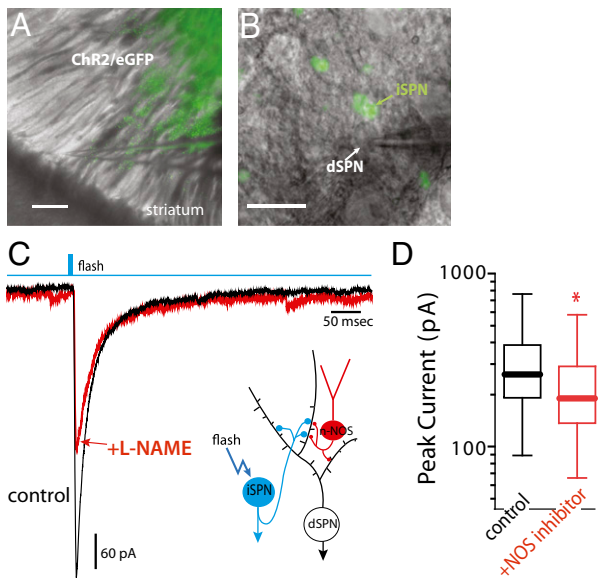
**Fig. 4.** Disruption of NO signaling reduces iSPN collateral input onto dSPNs. (*A*) Striatal cells (iSPNs) transfected by viral delivery of channel rhodopsin (ChR2, coexpressing YFP) are shown in green overlaid on the corresponding differential interference contrast image of a 200-µm sagittal brain slice. (Scale bar: 250 µm.) (*B*) A magnified view of the region around the recording pipette seen in *A*. (Scale bar: 100 µm.) Note the proximity of a transfected iSPN to the recorded, nontransfected dSPN. (*C*) Representative traces show the response of the recorded dSPN to GABAergic iSPN collateral input generated by a 200-µs duration pulse of 470 nm wavelength light delivered via an LED light source. The vertical tick in the bar above the traces indicates the onset of the light pulse (not to scale). The traces represent the average of ~8–10 responses before (control) and after (L-NAME) a 12-min incubation in the NOS inhibitor, L-NAME (100 µM). The glutamate receptor antagonists APV [(2R)-amino-5-phosphonovaleric acid; (2R)-amino-5-phosphonopenta-noate] (50 µM) and DNQX (6,7-dinitroquinoxaline-2,3-dione, 10 µM) were present throughout the experiment. (Inset) A simplified schematic of striatal circuitry indicating the collateral innervations being examined. (*D*) A summary of the data obtained from a set of 13 cells in experiments as outlined in *C*. The absolute amplitudes of the GABAergic responses before and after L-NAME treatment are represented as box plots demonstrating median value and interquartile range. Amplitudes were statistically analyzed using the Mann–Whitney *U* test (*$P < 0.05$).

nuclear or cytoplasmic levels of PKG1 (Fig. 5 *E* and *F*), suggesting that the activity of PKG1 in the nucleus is not dependent on its nuclear shuttling. In sGCβ1 KD mice, the level of PKG1 was reduced in the nucleus (70 ± 6% of control) and the cytoplasm (74 ± 10% of control) (Fig. S5), supporting the idea that the activity of PKG1 in the nucleus may play a role in the transcriptional regulation by NO.

Finally, to study a direct interaction between CREB and regulatory elements in the VGAT gene, the sequence of the VGAT gene (*Slc32a1*) was analyzed, and a conserved cAMP response element (CRE) was identified in its intron (Fig. S5). To evaluate the functionality of this putative CRE, the binding of *VGAT* to CREB was studied in vitro. A specific interaction was identified between phospho-CREB and the *vgat* gene (Fig. S5). Moreover, this interaction was dependent on the CRE-like sequence, suggesting that it is functional. To evaluate a possible interaction between *vgat* and phospho-CREB in vivo, chromatin from either the striatum or hippocampus was isolated, and levels of the gene bound to either phospho-CREB or RNA polymerase II were assessed using chromatin immunoprecipitation (i.p.) and qPCR. The levels of *vgat* precipitated by RNA Polymerase were 4 ± 1.0% and 1.2 ± 0.2% of the striatal and hippocampal gene inputs, respectively (*P* = 0.04 between brain areas), and the respective levels precipitated by phospho-CREB were 0.3 ± 0.07% and 0.08 ± 0.01%, respectively (*P* = 0.02 between brain areas),

suggesting that CREB plays a role in the transcriptional regulation of VGAT in striatal neurons. Importantly, in striata of sGCβ1 KD mice, the binding of *vgat* by phospho-CREB was reduced by 56 ± 8.7% (Fig. 5*G*), indicating that CREB-induced transcriptional regulation of *vgat* is attenuated in sGCβ1 KD mice.

**Dopamine Signaling Regulates Striatal cGMP and Collateral VGAT Levels in a Coordinated Manner.** Striatal dopamine depletion is associated with impairments in both striatal NO signaling and GABAergic transmission in axon collaterals of SPNs (14, 19). To study the role of dopamine in the regulation of striatal NO signaling and VGAT levels in SPNs, cGMP levels or VGAT labeling was measured in the striata from 6-hydroxydopamine lesioned mice (Fig. 6*A*). Dopaminergic denervation resulted in a 21 ± 6% reduction in VGAT labeling from the striatum ipsilateral to the lesion (Fig. 6 *B* and *C*). The reduction in VGAT level was observed both in the neuropil and somas of SPNs. In contrast to the reduction at local processes of SPNs, the level of VGAT at extrastriatal projections to the globus pallidus and substantia nigra was not affected by the lesion (Fig. S6), indicating that dopamine transmission modulates VGAT levels only at recurrent axon collaterals but not at primary projections of SPNs. Chronic L-dopa treatment increased striatal VGAT labeling by 37 ± 12% whereas discontinuation of L-dopa resulted in a 33 ± 11% reduction in the transporter level.

Dopamine depletion also resulted in a 53 ± 5% reduction in cGMP levels in the striatum ipsilateral to the lesion (ipsilateral 2.2 ± 0.5 pmol/mg wet weight; contralateral 4.5 ± 0.7 pmol/mg wet weight) (Fig. 6*D*). Chronic L-dopa treatment increased cGMP levels by 46 ± 11% (5.4 ± 0.9 pmol/mg wet weight; 3.7 ± 0.5 pmol/mg wet weight) whereas its withdrawal resulted in a 49 ± 14 pmol/mg wet weight loss in cGMP levels (2.0 ± 0.5 pmol/mg
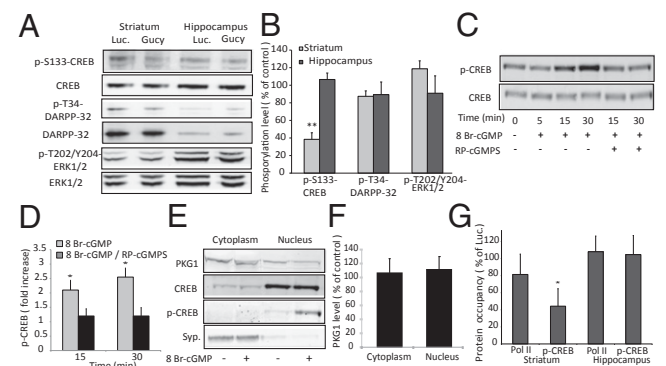


**Fig. 5.** Transcriptional regulation of VGAT by NO signaling. (*A*) Representative immunoblot image of phosphoproteins from control (*n* = 4 mice) and sGCβ1 KD (*n* = 4 mice). (*B*) Quantification of the data presented in *A*, indicating a reduction in phospho-CREB levels in the striata of sGCβ1 KD mice (**$P = 0.006$). Bars represent means of phosphorylated fraction ± SD. (*C* and *D*) Effect of cGMP on subcellular levels of PKG1 in striatal slices. (*C*) Representative Western blot images of Ser-133 phospho-CREB and total CREB levels, after incubation of striatal slices with 8 Br-cGMP (cGMP analog, 5 µM), RP-cGMPS (PKG1α selective inhibitor, 1 µM, *n* = 6 slices per group). (*D*) Quantification of the data presented in *C*, showing induction in CREB-phosphorylation by 8 Br-cGMP alone but not with RP-cGMPS (*$P < 0.05$ vs. 8 Br-cGMP/RP-cGMPS). Bars represent means of fold change in phosphorylated fraction relative to time 0 ± SD. (*E*) Representative Western blot image depicting protein subcellular levels after 30 min incubation of striatal slices with 8 Br-cGMP. (*F*) Bar graph summary of the data presented in *E*, indicating that the induction of CREB phosphorylation by 8 Br-cGMP is not associated with nuclear translocation of PKG1 (5 µM, *n* = 3 mice, six slices from each, per group). (*G*) Impaired interaction between CREB and *vgat* gene in sGCβ1 KD mice. Bar graph summary of the striatal levels of *vgat* (*slc32a1*), bound by either S133-phospho-CREB or RNA polymerase II. The level of bound genes from control (*n* = 10) or sGCβ1 KD (*n* = 10) was analyzed using qPCR. Bars represent mean levels of the immunoprecipitated gene in sGCβ1 KD mice normalized to input, as percentage of control ± SD (*$P < 0.05$).
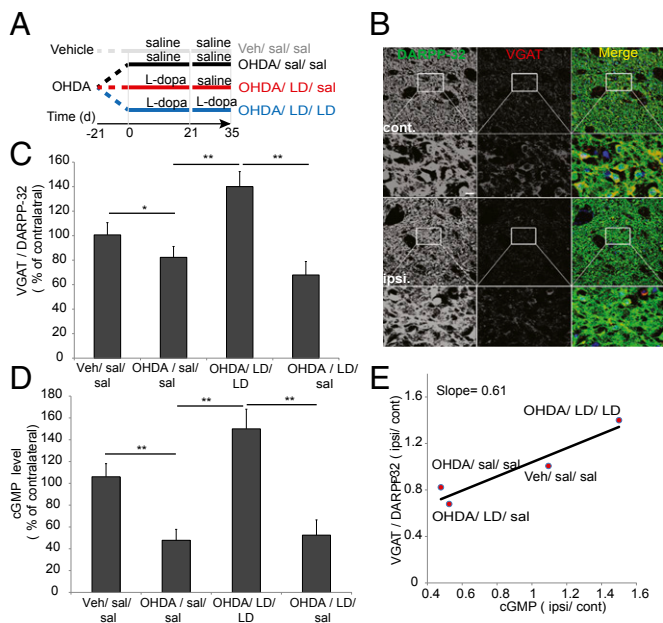
**Fig. 6.** Coregulation of VGAT and cGMP levels by dopamine. (*A*) Dopaminergic lesion paradigm. Mice received a unilateral injection of either 6-hydroxydopamine (OHDA) or vehicle to the medial forebrain bundle and daily intraperitoneal injections of benseazide (15 mg/kg) with L-dopa (6 mg/kg, LD) or saline (sal). (*B*) VGAT and DARPP-32 immunolabeling in the striatum after dopaminergic lesion. Representative images from ipsilateral (ipsi.) and contralateral (cont.) striatum of a mouse treated with 6-hydroxydopamine and saline. Note in the magnified images that VGAT labeling (shown in yellow in the image from the contralateral) is reduced in the soma of SPNs of the ipsilateral striatum (appears green). (Scale bar: 20 μm.) (*C*) Bar graph summary of ratios of VGAT and DARPP-32 mean pixel values (*n* = 5–6 mice per group, seven slices per mouse). Bars represent mean ratios in the ipsilateral striatum as percentage of that in the contralateral ± SD. (*D*) cGMP levels. Bars represent cGMP level in the ipsilateral striatum normalized to tissue wet weight, as percentage of the contralateral ± SD (*n* = 4–5 mice per group). (*E*) For each treatment group, the mean cGMP level is plotted against the mean of VGAT labeling ratio.

wet weight; $3.9 \pm 1.0$ pmol/mg wet weight). Finally, a correlation between the regulation of cGMP and VGAT levels by dopamine was evaluated by plotting striatal cGMP level changes against that of local VGAT labeling. High correlation was identified between the two ($R^2 = 0.903$) (Fig. 6*E*), further supporting the idea that striatal NO mediates the dynamic regulation of axon collateral function in SPNs by dopaminergic signaling.

## Discussion

NO signaling has an established role in mediating plasticity and transmission in excitatory synapses, including a role in striatal plasticity at corticostriatal synapses, where it facilitates the response of SPNs to glutamate (6, 7). We have previously found that the NO-sGC-cGMP pathway regulates striatal glutamate signaling through NMDA/AMPA/mGluR5 receptor activation. To identify the molecular mechanisms underlying the role of NO in SPNs, we have used the novel BacTRAP technology. We demonstrated that a loss of NO signaling from striatal neurons of the adult mouse striatum results in a specific reduction in the translated mRNA level of synaptic vesicle-related genes and an impaired GABAergic transmission at recurrent axon collaterals of striatal SPNs. By using a striatal-specific sGCβ1 KD strategy, we have found that transcriptional regulation of VGAT is a major target of NO-sGC signaling, establishing a mechanism by which this signaling pathway can trigger synaptic transmission at GABAergic local synapses. Importantly, we found that SPNs of the two projection pathways, namely the direct and the indirect pathways, are both targets of striatal NO signaling. sGCβ1 mRNA

was reduced in dSPN by a similar level to that of the entire striatal tissue, suggesting that the effect is similar in iSPNs. Furthermore, immunolabeling of VGAT was reduced by a similar ratio in both populations in sGCβ1-KD.

Interestingly, sGCβ1-KD mice manifested induction in motor behavior, highlighting asymmetry in the role of NO on local communication between the projection systems. This result suggests that iSPN neurons are more sensitive to the transcriptional regulation of VGAT by NO than dSPNs. In line with this idea, we and others have previously found that axon collaterals between SPNs of the two projection systems are not symmetrical because iSPNs profoundly innervate and efficiently inhibit dSPNs (14, 20, 21). Together with these studies, our experiments suggest that NO signaling regulates motor behavior and action selection by maintaining the normal function of axon collaterals.

We found that cGMP, sGC, PKG1, and CREB are involved in the signaling pathway that transcriptionally regulates VGAT by NO. PKG1 is localized both to the cytoplasm and to the nucleus, and its nuclear levels are reduced in sGCβ1 KD mice, suggesting that PKG1 directly regulates the transcription of downstream genes by phosphorylating nuclear targets, including transcription factors. This finding is in line with the fact that PKG1 can directly phosphorylate CREB (22). By using acute slices, we found that phosphorylation of CREB by cGMP in striatal neurons depends on PKG1, suggesting that protein translation of VGAT at local striatal synapses is unlikely to mediate the transcriptional regulation by NO signaling. Induction in CREB phosphorylation can induce transcriptional activation through binding to the CRE element in target genes (22). In line with this idea, we found a functional CRE in the VGAT gene and identified a loss in the phosphorylation level of CREB and in its binding to the VGAT gene in sGCβ1 KD mice, indicating that CREB positively regulates their transcription. Whether transcriptional regulation of vesicular neurotransmitter transporters is always coordinated with that of other presynaptic and vesicular genes is still unknown. We found that, in contrast to VGAT, only a small subset of other presynaptic genes were differentially expressed in SPNs of sGCβ1 KD mice. Previous work in cultured neurons showed that the transcriptional regulation of VGAT and other vesicular neurotransmitters transporters is dissociated from that of other components of the synaptic vesicle (23), and our results indicate that such selective regulation is maintained in the adult mammalian brain.

The loss of response of neurons transduced with AAV.si.Gucy to the NO donor diethylamine NONOate confirmed that NO signaling is impaired in sGC-KD mice. Similar to NO, carbon monoxide (CO) is another gaseous neurotransmitter and a ligand for sGC (24). However, CO affinity to sGC is much lower than that of NO, and cGMP induction by CO is significantly lower relative to NO (25). Furthermore, the expression of heme oxygenase isoforms in the striatum is miniscule whereas basal cGMP level in the striatum is the highest in the brain. Taken together, it is likely that the activity of sGC in its role in mediating GABA transmission and plasticity is primarily regulated by NO. In contrast to sGCβ1 KD, the mechanism underlying the reduction in GABA signaling in SPN collaterals after pharmacologic inhibition of NOS may not depend on transcriptional regulation, suggesting that multiple mechanisms mediate the effect of NO on GABA transmission. Several mechanisms have been proposed in the action of NO on GABA transmission and plasticity, including some that are independent of sGC (1, 2). To identify sGC-dependent effects of NO, we down-regulated sGC in striatal neurons. In line with our previous reports showing that sGC and cGMP mediate NO signaling in SPNs (6, 12), the down-regulation of VGAT levels and the impairment in GABA signaling in sGCβ1 KO clearly indicate that sGC plays a major role in the function of axon collaterals of SPNs. The reduction in cGMP levels in response to application of NO donor after loss of sGC in cultured neurons further supports the idea that sGC is a major target of NO. However, a role for NO that is independent of sGC in mediating GABA transmission cannot be

completely ruled out. S-nitrosylation of cysteines in multiple target proteins has long been suggested to mediate synaptic plasticity at excitatory synapses (26). Interestingly, S-nitrosylation of gephrin by NO was recently shown to mediate GABA-A receptor assembly, suggesting that NO may regulate synaptic plasticity at GABAergic synapses independently of sGC (27). It is therefore possible that L-NAME–mediated inhibition of GABA signaling was mediated by changes in S-nitrosylation and that sGC-dependent and independent mechanisms by NO are activated in a coordinated manner on both sides of the GABAergic synapse to mediate GABA signaling and synaptic plasticity.

The reduction in VGAT mRNA level in sGCβ1 KD mice resulted in a parallel reduction in the level of the protein. Interestingly, the reduction in VGAT protein level in sGCβ1 KD mice was found only in local processes of SPNs but not in their primary projections. Similarly, the reduction in GABA transmission was found specifically at axon collaterals of SPNs, but not in their primary extrastriatal terminals. Differences in regulation of the level of VGAT or in its trafficking between these two types of terminals have not been reported yet, but several mechanisms may underlay these differences. Cytoskeletal proteins, including kinesin motors, which mediate trafficking of synaptic content, may play a role in the function of axon collaterals (28). Among the members of this protein superfamily, kinesin 2A and 5 were previously shown to mediate a specific suppression of collateral-branch extension (29, 30). Interestingly, we identified an up-regulation in the level of these proteins, as well as down-regulation in the level of several other kinesin members (Table S1). Still, the exact function and cellular distribution of each member of the kinesin protein family in SPNs is not known, and further work will be necessary to elucidate their function and regulation in axon collaterals of SPNs.

## Materials and Methods

A full description of the materials and methods can be found in *SI Materials and Methods*.

**Animals.** Experiments were performed in accordance with National Institutes of Health guidelines for the care and use of laboratory animals, and all procedures were carried out in accordance with the National Institutes of Health *Guide for the Care and Use of Laboratory Animals* (31), and were approved by the Animal Care and Use Committees of the Rockefeller University, the Weill Medical College of Cornell University, and the Feinberg School of Medicine, Northwestern University. For viral injections, 7-wk-old mice (or 5-wk-old mice for electrophysiology studies) were anesthetized with ketamine/xylazine and were bilaterally injected with 1.5 μL of AAV into the dorsal striatum using a mouse atlas-integrated stereotaxic instrument (Leica). Coordinates were ±2.05 mm, +0.25 mm, −3.96 mm lateral, anterior, and ventral from bregma according to the Paxinos and Franklin mouse brain atlas (2001) (32). Unless specified otherwise, assessment of the effect of the AAV was performed at 25 ± 3.2 d after injections in lysates of striata that were dissected between anterior + 0.38 and 0.00, relative to bregma. All other in vivo studies are described in *SI Materials and Methods*.

**RNA Isolation, Purification, and Analysis.** Striata and brainstems from six Drd1-bacTRAP mice (CP-73), both males and females, were pooled to isolate RNA. RNA was isolated as previously shown (10, 11).

1. Li DP, Chen SR, Finnegan TF, Pan HL (2004) Signalling pathway of nitric oxide in synaptic GABA release in the rat paraventricular nucleus. *J Physiol* 554(Pt 1):100–110.
2. Nugent FS, Penick EC, Kauer JA (2007) Opioids block long-term potentiation of inhibitory synapses. *Nature* 446(7139):1086–1090.
3. Garthwaite J (2008) Concepts of neural nitric oxide-mediated transmission. *Eur J Neurosci* 27(11):2783–2802.
4. Ding JD, Burette A, Nedvetsky PI, Schmidt HH, Weinberg RJ (2004) Distribution of soluble guanylyl cyclase in the rat brain. *J Comp Neurol* 472(4):437–448.
5. Matsuoka I, et al. (1992) Localization of adenylyl and guanylyl cyclase in rat brain by in situ hybridization: Comparison with calmodulin mRNA distribution. *J Neurosci* 12(9):3350–3360.
6. Nishi A, et al. (2005) Glutamate regulation of DARPP-32 phosphorylation in neostriatal neurons involves activation of multiple signaling cascades. *Proc Natl Acad Sci USA* 102(4):1199–1204.
7. Calabresi P, et al. (1999) A critical role of the nitric oxide/cGMP pathway in corticostriatal long-term depression. *J Neurosci* 19(7):2489–2499.
8. Echeverry MB, Salgado ML, Ferreira FR, da-Silva CA, Del Bel EA (2007) Intracerebroventricular administration of nitric oxide-sensitive guanylyl cyclase inhibitors induces catalepsy in mice. *Psychopharmacology (Berl)* 194(2):271–278.
9. Stewart J, Deschamps SE, Amir S (1994) Inhibition of nitric oxide synthase does not block the development of sensitization to the behavioral activating effects of amphetamine. *Brain Res* 641(1):141–144.
10. Heiman M, et al. (2008) A translational profiling approach for the molecular characterization of CNS cell types. *Cell* 135(4):738–748.
11. Doyle JP, et al. (2008) Application of a translational profiling approach for the comparative analysis of CNS cell types. *Cell* 135(4):749–762.
12. Tsou K, Snyder GL, Greengard P (1993) Nitric oxide/cGMP pathway stimulates phosphorylation of DARPP-32, a dopamine- and cAMP-regulated phosphoprotein, in the substantia nigra. *Proc Natl Acad Sci USA* 90(8):3462–3465.
13. Harvey VL, Stephens GJ (2004) Mechanism of GABA receptor-mediated inhibition of spontaneous GABA release onto cerebellar Purkinje cells. *Eur J Neurosci* 20(3):684–700.
14. Taverna S, Ilijic E, Surmeier DJ (2008) Recurrent collateral connections of striatal medium spiny neurons are disrupted in models of Parkinson's disease. *J Neurosci* 28(21):5504–5512.
15. Tepper JM, Wilson CJ, Koós T (2008) Feedforward and feedback inhibition in neostriatal GABAergic spiny neurons. *Brain Res Brain Res Rev* 58(2):272–281.
16. Kuroda S, Schweighofer N, Kawato M (2001) Exploration of signal transduction pathways in cerebellar long-term depression by kinetic simulation. *J Neurosci* 21(15):5693–5702.
17. Pozzi L, et al. (2003) Opposite regulation by typical and atypical anti-psychotics of ERK1/2, CREB and Elk-1 phosphorylation in mouse dorsal striatum. *J Neurochem* 86(2):451–459.
18. Gudi T, et al. (2002) cGMP-dependent protein kinase inhibits serum-response element-dependent transcription by inhibiting rho activation and functions. *J Biol Chem* 277(40):37382–37393.
19. Giorgi M, et al. (2008) Lowered cAMP and cGMP signalling in the brain during levodopa-induced dyskinesias in hemiparkinsonian rats: New aspects in the pathogenetic mechanisms. *Eur J Neurosci* 28(5):941–950.
20. Wall NR, De La Parra M, Callaway EM, Kreitzer AC (2013) Differential innervation of direct- and indirect-pathway striatal projection neurons. *Neuron* 79(2):347–360.
21. Planert H, Szydlowski SN, Hjorth JJ, Grillner S, Silberberg G (2010) Dynamics of synaptic transmission between fast-spiking interneurons and striatal projection neurons of the direct and indirect pathways. *J Neurosci* 30(9):3499–3507.
22. Rogge GA, Shen LL, Kuhar MJ (2010) Chromatin immunoprecipitation assays revealed CREB and serine 133 phospho-CREB binding to the CART gene proximal promoter. *Brain Res* 1344:1–11.
23. De Gois S, et al. (2005) Homeostatic scaling of vesicular glutamate and GABA transporter expression in rat neocortical circuits. *J Neurosci* 25(31):7121–7133.
24. Stone JR, Marletta MA (1994) Soluble guanylate cyclase from bovine lung: Activation with nitric oxide and carbon monoxide and spectral characterization of the ferrous and ferric states. *Biochemistry* 33(18):5636–5640.
25. Derbyshire ER, Marletta MA (2012) Structure and regulation of soluble guanylate cyclase. *Annu Rev Biochem* 81:533–559.
26. Huang Y, et al. (2005) S-nitrosylation of N-ethylmaleimide sensitive factor mediates surface expression of AMPA receptors. *Neuron* 46(4):533–540.
27. Dejanovic B, Schwarz G (2014) Neuronal nitric oxide synthase-dependent S-nitrosylation of gephyrin regulates gephyrin clustering at GABAergic synapses. *J Neurosci* 34(23):7763–7768.
28. Takamori S, et al. (2006) Molecular anatomy of a trafficking organelle. *Cell* 127(4):831–846.
29. Homma N, et al. (2003) Kinesin superfamily protein 2A (KIF2A) functions in suppression of collateral branch extension. *Cell* 114(2):229–239.
30. Myers KA, Baas PW (2007) Kinesin-5 regulates the growth of the axon by acting as a brake on its microtubule array. *J Cell Biol* 178(6):1081–1091.
31. National Research Council (2011) *Guide for the Care and Use of Laboratory Animals* (National Academies Press, Washington, DC), 8th Ed.
32. Paxinos G, Franklin KBJ (2001) *The Mouse Brain in Stereotaxic Coordinates* (Academic, San Diego).

NEUROSCIENCE